Identifying an Environment-Induced Localization Transition from Entropy and Conductance

Zhanyu Ma,[1] Cheolhee Han,[1] Yigal Meir,[2] and Eran Sela[1]
[1]*School of Physics and Astronomy, Tel Aviv University, Tel Aviv 6997801, Israel*
[2]*Department of Physics, Ben-Gurion University of the Negev, Beer-Sheva 84105, Israel*

(Received 13 April 2023; accepted 5 September 2023; published 22 September 2023)

Environment-induced localization transitions (LT) occur when a small quantum system interacts with a bath of harmonic oscillators. At equilibrium, LTs are accompanied by an entropy change, signaling the loss of coherence. Despite extensive efforts, equilibrium LTs have yet to be observed. Here, we demonstrate that ongoing experiments on double quantum dots that measure entropy using a nearby quantum point contact realize the celebrated spin-boson model and allow to measure the entropy change of its LT. We find a Kosterlitz-Thouless flow diagram, leading to a universal jump in the spin-bath interaction, reflected in a discontinuity in the zero temperature QPC conductance.

DOI: 10.1103/PhysRevLett.131.126502

Introduction.—Environment-induced localization transitions (LTs) occur when a small quantum system switches from coherent to incoherent dynamics due to its interaction with an infinite number of environmental degrees of freedom. A simple example of this is the spin-boson model [1,2]. It was proposed already 40 years ago [3–5] that when the coupling of the spin or two-level system to the bath exceeds a certain threshold, the tunneling between the two levels vanishes. Despite numerous proposals to observe this phase transition in various mesoscopic [6–9] and atomic [10,11] systems, or by tracking the dynamics of the quantum system [11], this LT has not been observed to date without external driving [12]. This is largely due to the experimental difficulty of continuously tuning the coupling or altering the power-law spectrum of the bosonic bath. Different than dissipative phase transitions [13–18] that occur out of equilibrium, LTs can be identified in their thermodynamic properties. Here, utilizing the fact that the entropy displays a characteristic change across the transition [19] we demonstrate that already existing experimental setups measuring the entropy of quantum dot (QD) systems [20–22] can be employed to observe the hitherto elusive LT for the spin-boson model at equilibrium.

Our proposed realization of the two-level system is a double dot (DD) containing a single electron, having a pair of states denoted $\{|01\rangle, |10\rangle\}$, with the electron being in the right or left QD, respectively (the spin of the electron is irrelevant). The role of the bath is played by a nearby quantum point contact (QPC), whose transmission is controlled by gate voltage V_g, which acts as a charge detector [23] of QD A, see Fig. 1(a). Below, we relate the QPC QD electrostatic coupling to an effective change of the scattering phase shift δ in the QPC, occurring as an electron enters QD A.

The decoupled system ($\delta = 0$) undergoes a $k_B \log 2$ entropy drop (where k_B is the Boltzmann constant, set to unity in the following) as the temperature is lowered below the DD tunneling amplitude w. Indeed, the symmetric DD

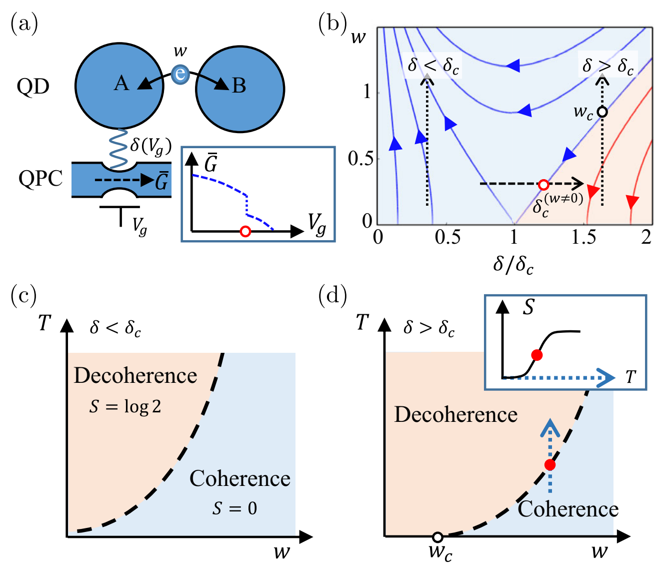

FIG. 1. (a) Model: quantum dot (QD) A tunnel coupled (via w) to QD B, here another QD, and electrostatically coupled (as parametrized by δ) to a quantum point contact (QPC). δ is tuned by a gate voltage V_g and $\bar{G}$ is the average QPC conductance. The inset shows a conductance jump obtained by changing $V_g(\delta)$. (b) RG flow diagram. In the red (blue) shaded area, δ flows to $\delta \neq 0$ ($\delta = 0$). Two black dotted lines correspond to the w axis of (c) and (d) and the black dashed line corresponds to the V_g axis of the inset of (a). (c) At $\delta < \delta_c$, there is no quantum phase transition tuned by w. (d) For $\delta > \delta_c$ at $T = 0$, there appears a LT at $w = w_c$ (empty circle), characterized by an entropy jump.

transitions from the high-temperature state, described by the diagonal density matrix $(|01\rangle\langle 01| + |10\rangle\langle 10|)/2$, to the coherent ground state $(|01\rangle + |10\rangle)/\sqrt{2}$. We predict that for a nonzero coupling to the bath, $\delta > 0$, the temperature scale for this incoherent-coherent crossover decreases, and eventually vanishes at the LT at some $\delta = \delta_c$. This can be understood from the Anderson orthogonality catastrophe [9,24,25]. For $\delta > \delta_c$ the orthogonality between the many-body wave functions of the QPC for the QD states $|01\rangle$ and $|10\rangle$ effectively turns the tunneling amplitude w to zero, see Figs. 1(b) and 1(d), reminiscent of the Zeno effect [26,27], and the entropy remains log2 down to zero temperature. We find that both w and the effective electrostatic interaction δ are scaling variables of the LT described by the renormalization group (RG) flow diagram of a Kosterlitz-Thouless (KT) transition, see Fig. 1(b). While it may be difficult to tune δ, the LT can be driven as a function of tunneling coupling w, which can be readily tuned by a gate. As seen in Fig. 1(d) there is a critical tunneling amplitude w_c below which the entropy remains finite at zero temperature, while coherence develops for $w > w_c$, manifested as a drop of the entropy to zero at low temperature.

From this flow diagram, we can see that the effective QPC QD interaction $\delta_{\rm eff}$ at low temperature, being the destination of the flow diagram, changes discontinuously depending on its bare value, between a finite value $\delta_{\rm eff} \geq \delta_c$ in the incoherent phase, and $\delta_{\rm eff} = 0$ in the coherent phase. This universal step is the analog of the discontinuity in the superfluid density in the standard KT transition due to vortices. In our system, unexpectedly, this is reflected as a sudden change of the QPC conductance as $T \to 0$, see inset of Fig. 1(a).

Model.—As depicted in Fig. 1(a), we consider a DD electrostatically coupled to a QPC with Hamiltonian $H = H_{\rm DD} + H_{\rm QPC}$. $H_{\rm DD}$, defined explicitly in Eq. (6) below, describes two subsystems. Subsystem A is a QD in the Coulomb blockade regime which accommodates only two charge states labeled by $N_A = 0,\ 1$, while subsystem B could be, in principle, arbitrary. For simplicity, we consider here the case when the subsystem B is another QD (for more examples, see [28]). The two subsystems are connected via a tunneling amplitude w. We use the Pauli matrix $\sigma^z = |1\rangle\langle 1| - |0\rangle\langle 0|$ to denote the charge operator of QD A, $\hat{N}_A = (1+\sigma^z)/2$. For the symmetric DD system, $H_{\rm DD} = w\sigma^x$.

The QPC consists of a quantum wire running along the x direction, interrupted by a potential barrier $V_{N_A}(x,y)$,

$$H_{\rm QPC} = \int dxdy \sum_{s=\uparrow,\downarrow} \Psi_s^\dagger(x,y)\bigg[-\frac{\hbar^2}{2m}\nabla^2 + V_0(x,y)|0\rangle\langle 0| + V_1(x,y)|1\rangle\langle 1|\bigg]\Psi_s(x,y). \quad (1)$$

As a consequence, the potential in the QPC suddenly switches between $V_1(x,y)$ and $V_0(x,y)$ as an electron tunnels in and out of QD A. An explicit model for $H_{\rm QPC}$ is considered below in Eq. (9) where $V_{N_A}(x,y) = V(y) + V_{N_A}(x)$, with $V_{N_A}(x) = V_{N_A}(-x)$. In this case, for each transverse mode $n = 0, 1, 2, \ldots$ of the potential $V(y)$ the scattering matrix is diagonal and encoded by the even and odd phase shifts $\delta_{N_A}^{(e,n)}, \delta_{N_A}^{(o,n)}$. For more general cases see [28]. For convenience, we label parity, channel, and spin index collectively by a single index $i = \{e/o, n, s\} = 1, \ldots, i_{\max}$, and also define the difference and average phase shifts in each channel $\delta_i = (\delta_0^i - \delta_1^i)/2$ and $\bar{\delta}_i = (\delta_0^i + \delta_1^i)/2$.

Mapping to the spin-boson model.—At energies close to the Fermi energy, the fermion fields $\psi_{n,s}(x)$ have left and right components [34,35], $\psi_{n,s}(x) = e^{ik_{F,n}x}\psi_{R,n,s} + e^{-ik_{F,n}x}\psi_{L,n,s}$. It allows us to define even and odd chiral fields $\psi_{e/o,n,s} = [\psi_{R,n,s}(x) \pm \psi_{L,n,s}(-x)]/\sqrt{2}$ which we bosonize [36] into

$$H_{\rm QPC} = v_F \sum_i \left(\int \frac{dx}{4\pi}(\partial_x\phi_i)^2 - \frac{\delta_i}{\pi}\sigma^z\partial_x\phi_i(0)\right) + H_{ps}, \quad (2)$$

with $[\phi_j(x), \partial_y\phi_k(y)] = -2\pi i\delta_{jk}\delta(x-y)$ [36]. The second term $\propto \sigma_z$ describes the N_A-dependent potential. The last term $H_{ps} = -(v_F/\pi)\sum_i \bar{\delta}_i\partial_x\phi_i(0)$ is a constant potential that can be removed by a unitary transformation $H \to UHU^\dagger$ with $U = e^{-i\sum_j \bar{\delta}_j\phi_j(0)/\pi}$. We define

$$\delta = \sqrt{\sum_i \delta_i^2}, \quad (3)$$

and $\phi(x) = (1/\delta)\sum_i \delta_i\phi_i(x)$, along with $i_{\max} - 1$ orthogonal combinations $\{\phi_i', i = 2, \ldots, i_{\max}\}$ which do not interact with σ^z. We obtain $H = H_{\rm eff}(\phi) + \sum_{i=2}^{i_{\max}} H[\phi']$ where the LT is captured by the effective model

$$H_{\rm eff}(\phi) = \frac{v_F}{4\pi}\int dx(\partial_x\phi)^2 - \frac{v_F}{\pi}\delta\sigma^z\partial_x\phi(0) + w\sigma^x. \quad (4)$$

This model is equivalent to the spin-boson model with an Ohmic bath [28]. The term $\propto \delta\sigma^z$ describes the interaction between the spin and the bosonic environment $\phi(x)$.

Anderson orthogonality catastrophe and LT.—One can apply a similar transformation $U' = e^{i\sigma^z\delta\phi(0)/\pi}$ to remove the interaction $\propto \delta\sigma^z$ from Eq. (4). Then the tunneling term $\propto w\sigma^+ + \mathrm{H.c.}$ gets "dressed" by a bath operator known as a boundary condition changing operator with scaling dimension $x_b = 2(\delta/\pi)^2$ [9,34]. It reflects the orthogonality of the many-body ground states of the QPC for $N_A = 0, 1$. Thus, the tunneling w satisfies the RG equation $dw/dl = w(1 - x_{\rm tun} - x_b)$ where $x_{\rm tun} = 0$ is the bare scaling dimension of w. More generally, we find [28]

$$\frac{dw}{dl} = w\left[1 - \left(\frac{\delta}{\delta_c}\right)^2\right], \qquad \frac{d\delta}{dl} = -2\delta w^2, \quad (5)$$

where $\delta_c = \pi/\sqrt{2}$ for the DD. For small enough w, we see that w switches, upon increasing δ, from being relevant to irrelevant at $\delta = \delta_c$. This critical interaction separates the strong interaction phase $\delta > \delta_c$ in which the coherent tunneling is suppressed as in the Zeno effect, from the weak interaction phase $\delta < \delta_c$ with coherent tunneling. Equivalently, there is an energy scale that vanishes at the quantum phase transition [28,37] $T^* \approx w^{\pi^2/4\delta_c(\delta_c-\delta)}$. More generally, also δ flows according to the celebrated KT flow diagram in Fig. 1(b). For $\delta > \delta_c$ we deduce a LT as function of w, see Fig. 1(d). We now apply numerical renormalization group (NRG) calculations to demonstrate these signatures more quantitatively.

NRG results.—The spinless DD is described by

$$H_{\mathrm{DD}} = -\mu(a^\dagger a + b^\dagger b) + \Delta(a^\dagger a - b^\dagger b) - w(a^\dagger b + \mathrm{H.c.}) + U a^\dagger a b^\dagger b, \tag{6}$$

where μ and Δ denote, respectively, the DD chemical potential and asymmetry. As finite asymmetry smears the LT [28], we focus here on the symmetric case $\Delta = 0$. Here, $a(b)$ annihilates an electron in QD $A(B)$, $\hat{N}_A = a^\dagger a$ and we define the DD occupancy $N \equiv \langle a^\dagger a + b^\dagger b\rangle$. μ is used to continuously switch from the empty regime $N = 0$ to the singly occupied regime $N = 1$. We assume $U \to +\infty$ to exclude double occupancy. We ignore real spin, assuming that a particular electron spin is being trapped in the DD.

Our NRG calculations solve a fermionic lattice model corresponding to Eq. (1), which is also equivalent at low energy to the effective Hamiltonian Eq. (4) and hence reproduces its critical properties. It consists [28] of a fermionic semi-infinite tight binding chain interacting near the origin with the DD. The interaction term is selected [28] to yield the desired N_A-dependent phase shift δ. We compute the entropy, the total charge of the DD, and the many-body energy levels.

Figure 2(a) shows the entropy $S(T)$ in the singly occupied regime. We consider the interesting case with $\delta > \delta_c$. For $w > w_c$, $S(T)$ displays a drop by ln 2 below a characteristic energy scale T^* [defined as $S(T^*) = \frac{1}{2}\ln 2$]. As displayed in Fig. 2(b) by the thick blue curve, upon decreasing w, T^* decreases and eventually vanishes at $w = w_c(\delta)$. The precise form of the vanishing of T^* is shown in the inset, demonstrating the scaling behavior expected near the KT transition. The resulting phase diagram in Fig. 2(b), which is plotted for a few values of δ, has the structure of Fig. 1(c) for $\delta < \delta_c$ and Fig. 1(d) for $\delta > \delta_c$. In particular, for $\delta < \delta_c$, T^* only vanished at $w = 0$. Thus, the LT features a discontinuous change of entropy at $T \to 0$ as a function of w, see inset of Fig. 2(a).

Entropy from Maxwell relations.—Experimentally, changes in the entropy upon varying the DD chemical potential μ: $\mu_1 \to \mu_2$ are accessible via the Maxwell relation [20–22,38,39]

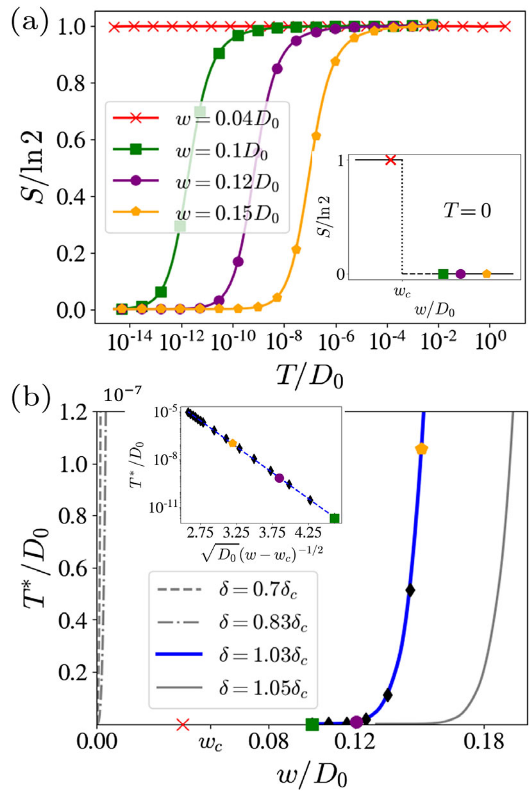

FIG. 2. (a) NRG results for the entropy versus T for various w and for $\delta = 1.03\delta_c$. For $w > w_c$ the entropy drops to zero at low temperatures, but for $w < w_c$ it remains ln 2 down to $T = 0$ as exemplified by the sudden change in the entropy at $T = 0$ at $w = w_c$, depicted in the inset. (b) Crossover temperature T^* for various δ as a function of w. The blue thick line corresponds to the parameter $\delta = 1.03\delta_c$ of (a), with the four colored markers denoting the crossover temperatures for the four different curves in (a). Inset: T^*/D_0 as a function of $D_0/(w - w_c)$, demonstrating the dependence $T^* \propto \exp[-\mathrm{const} \times (w - w_c)^{-1/2}]$, from which we extract w_c.

$$\Delta S_{\mu_1 \to \mu_2} = \int_{\mu_1}^{\mu_2} \frac{dN(\mu)}{dT} d\mu. \tag{7}$$

Namely, by using the QPC as a charge detector, one measures the differential charging curve dN/dT upon varying μ from the empty to the singly occupied regime. Since the entropy vanishes in the empty-DD regime, we obtain the entropy of the spin-boson model described by the singly occupied regime from this integral.

Figure 3 displays dN/dT as calculated from NRG (top panel) and the entropy change $S(\mu_2)$ as obtained by integration from $\mu_1 = -\infty$ to μ_2 (lower panel), for two different values of w, as shown in the inset of Fig. 3, at a fixed temperature. In the absence of the QPC, the ground state of the DD is unique (e.g., the symmetric state), and thus the entropy increases as a function of μ, from zero, in the empty-DD regime, to ln 2, when the empty and singly occupied states are degenerate and then decrease back to

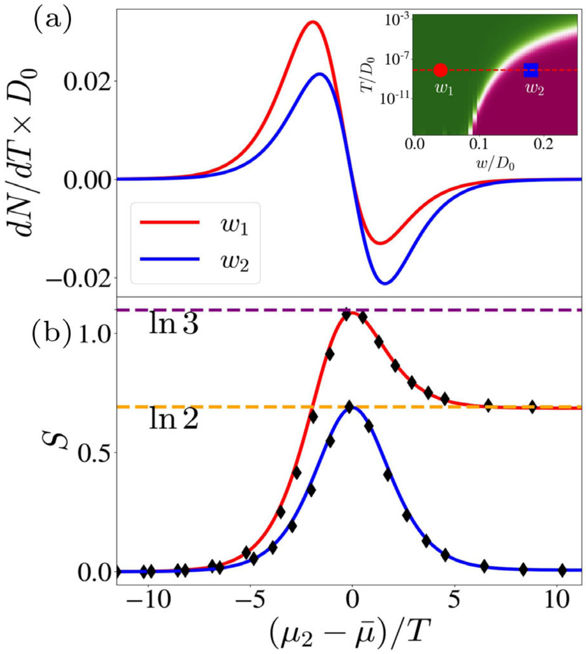

FIG. 3. (a) dN/dT for $\{w_1/D_0, w_2/D_0\} = \{0.03, 0.17\}$ as function of the DD chemical potential for $T/D_0 = 7.5 \times 10^{-9}$. Red (blue) lines describe the decoherence (coherence) phase, corresponding to the green (magenta) region as depicted in the inset. (b) Entropy $S(\mu_2)$ obtained by integrating dN/dT, see Eq. (7). We shifted the μ axis such that peaks occur at the origin. The blue curves for $w > w_c$ agree with the entropy of a decoupled DD, while for $w < w_c$ the system is driven to the incoherent phase. As a comparison, the black diamonds show the entropy obtained directly from NRG.

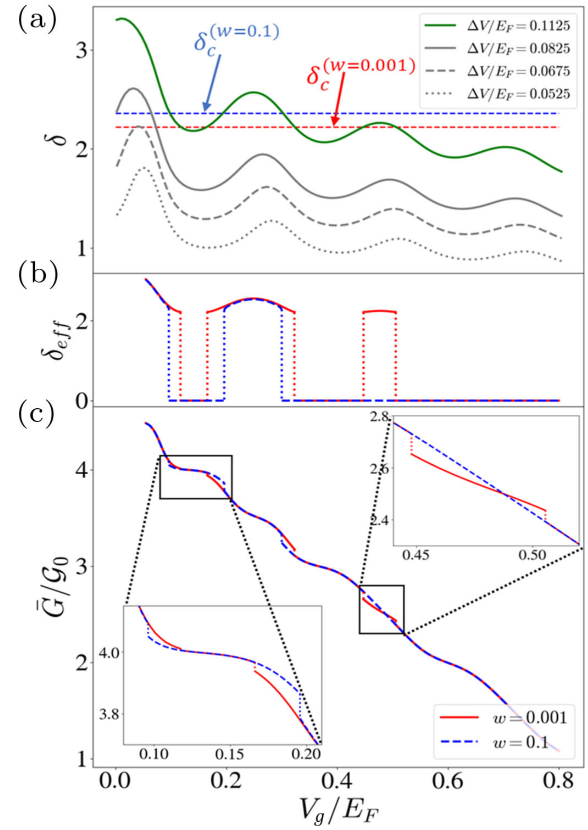

FIG. 4. (a) Phase shift δ for various electrostatic couplings ΔV, versus a gate voltage controlling the potential barrier [$E_F/\omega = 4.3$ and $\hbar^2/(2ma^2)/E_F = 100$]. Dashed horizontal lines denote $\delta_c^{(w)}$ for two values of w. (b) Renormalized phase shift $\delta_{\rm eff}$ for $\Delta V/E_F = 0.1125$ and $w/D_0 = 0.001$ (red) or $w/D_0 = 0.1$ (blue). Whenever δ crosses $\delta_c^{(w)}$ there is a discontinuous jump in $\delta_{\rm eff}$. (c) Corresponding conductance jumps.

zero in the singly occupied regime. This is observed when $w > w_c$ (blue curves). However, once w becomes smaller than w_c (or δ becomes larger than δ_c for this value of w), the behavior changes abruptly. Now, due to the loss of coherence between the two QDs, the two singly occupied states $|N = 1, N_A = 0, 1\rangle$ are degenerate, resulting in the increase of the entropy to ln 3 before dropping to ln 2 for the singly occupied state.

Conductance jump.—For a 2D superfluid, the Kosterlitz-Thouless RG equations result in a universal jump in the superfluid density [40]. What is then the corresponding discontinuous quantity in our system?.

The DD creates a different single-particle scattering potential on the QPC for each value of N_A. We can use the Landauer formula, which gives the conductance at $T = 0$

$$G_{N_A} = \frac{2e^2}{h} \sum_n \cos^2(\delta_{N_A}^{(e,n)} - \delta_{N_A}^{(o,n)}). \tag{8}$$

So a discontinuity in δ yields a discontinuity in G_{N_A}. To be concrete, consider the model

$$H_{\rm QPC} = -\frac{\hbar^2}{2m}(\partial_x^2 + \partial_y^2) + \frac{m\omega^2 y^2}{2} - \frac{\hbar\omega}{2} + \frac{V_0|0\rangle\langle 0| + V_1|1\rangle\langle 1|}{\cosh^2(x/a)}. \tag{9}$$

The Fermi momentum $k_{F,n}$ of the nth transverse mode satisfies $E_F = \hbar^2 k_{F,n}^2/2m + n\hbar\omega$ with $n = 0, 1, \ldots, \lfloor E_F/\omega \rfloor$. We let $V_0 = V_g$ and $V_1 = V_g + \Delta V$, with fixed ΔV characterizing the electrostatic interaction and a parameter V_g tunable using a gate voltage.

For each mode, one can analytically compute [41] the even and odd phase shifts, and thus obtain δ. In Fig. 4(a) we plot the calculated δ versus V_g for a constant ΔV for selected parameters corresponding to 5 transverse modes. Then δ displays peaks approximately when a transverse mode becomes reflecting. $\delta_c^{(w)}$ is marked by dashed lines for two values of w. In each case, we can see regions where $\delta > \delta_c^{(w)}$ are achieved for large enough ΔV.

From Fig. 1(b), one can see that upon increasing δ, as obtained by continuously varying V_g, when the condition

$\delta > \delta_c^{(w)}$ is met, the effective interaction $\delta(\ell \to \infty) \equiv \delta_{\rm eff}$ suddenly jumps from 0 to $\delta_c = \pi/\sqrt{2}$. In Fig. 4(b) we plot $\delta_{\rm eff}$ as extracted from the NRG finite-size spectrum [28], indeed demonstrating these sharp jumps.

For either the coherence or decoherence fixed points with $\delta \to 0$ or $w \to 0$, respectively, one can recombine the two terms $H = H_{\rm eff}(\phi) + \sum_{i=2}^{i_{\max}} H[\phi']$ by replacing $\delta \to \delta_{\rm eff}$. Returning to the original basis $\{\phi_i\}$, one can read off the even and odd phase shifts in each channel,

$$\left(\delta_{0,1}^{(i)}\right)_{\rm eff} = \bar{\delta}_i \pm \delta_i \frac{\delta_{\rm eff}}{\delta}. \qquad (10)$$

Substituting Eq. (10) in the expression (8) for the conductance, we see that when $\delta_{\rm eff}$ changes discontinuously across the LT, so do both G_0 and G_1. In Fig. 4(c) we plot the average conductance $\bar{G} = (G_0 + G_1)/2$ at $T = 0$. We see that it displays discontinuities precisely when the LT is crossed for each value of w (in Ref. [28] we show that a similar discontinuity can occur for a fixed V_g as a function of w). Thus, the LT of the KT type can be inferred from the conductance itself.

Summary.—Recent experiments demonstrated the ability to measure entropy changes in mesoscopic systems by coupling them to charge detectors. Here, we demonstrate that even at thermal equilibrium the charge detector may strongly affect the system and drive an environment-induced localization transition. The resulting entropy change describes the process of a quantum measurement of a state as it is being measured by an environment. Relating this entropy change due to measurement of a subsystem to entanglement entropy between the two subsystems is left for future work [42–44].

We gratefully acknowledge support from the European Research Council (ERC) under the European Unions Horizon 2020 research and innovation programme under Grant Agreement No. 951541. ARO (W911NF-20-1-0013) and the Israel Science Foundation Grant No. 154/19. We thank Josh Folk, Andrew Mitchell, and Sarath Sankar for discussions.

[1] Anthony J. Leggett, S. Chakravarty, Alan T. Dorsey, Matthew P. A. Fisher, Anupam Garg, and Wilhelm Zwerger, Dynamics of the dissipative two-state system, Rev. Mod. Phys. **59**, 1 (1987).

[2] Ulrich Weiss, *Quantum Dissipative Systems* (World Scientific, Singapore, 2012).

[3] Sudip Chakravarty, Quantum Fluctuations in the Tunneling Between Superconductors, Phys. Rev. Lett. **49**, 681 (1982).

[4] A. J. Bray and M. A. Moore, Influence of Dissipation on Quantum Coherence, Phys. Rev. Lett. **49**, 1545 (1982).

[5] Albert Schmid, Diffusion and Localization in a Dissipative Quantum System, Phys. Rev. Lett. **51**, 1506 (1983).

[6] Karyn Le Hur and Mei-Rong Li, Unification of electromagnetic noise and Luttinger liquid via a quantum dot, Phys. Rev. B **72**, 073305 (2005).

[7] Mei-Rong Li, Karyn Le Hur, and Walter Hofstetter, Hidden Caldeira-Leggett Dissipation in a Bose-Fermi Kondo Model, Phys. Rev. Lett. **95**, 086406 (2005).

[8] Ning-Hua Tong and Matthias Vojta, Signatures of a Noise-Induced Quantum Phase Transition in a Mesoscopic Metal Ring, Phys. Rev. Lett. **97**, 016802 (2006).

[9] Moshe Goldstein, Richard Berkovits, and Yuval Gefen, Population Switching and Charge Sensing in Quantum Dots: A Case for a Quantum Phase Transition, Phys. Rev. Lett. **104**, 226805 (2010).

[10] Alessio Recati, Peter O. Fedichev, Wilhelm Zwerger, Jan von Delft, and Peter Zoller, Atomic Quantum Dots Coupled to a Reservoir of a Superfluid Bose-Einstein Condensate, Phys. Rev. Lett. **94**, 040404 (2005).

[11] Diego Porras, F. Marquardt, J. Von Delft, and J. Ignacio Cirac, Mesoscopic spin-boson models of trapped ions, Phys. Rev. A **78**, 010101(R) (2008).

[12] Luca Magazzù, Pol Forn-Díaz, Ron Belyansky, J.-L. Orgiazzi, M. A. Yurtalan, Martin R. Otto, Adrian Lupascu, C. M. Wilson, and Milena Grifoni, Probing the strongly driven spin-boson model in a superconducting quantum circuit, Nat. Commun. **9**, 1 (2018).

[13] Eric M. Kessler, Geza Giedke, Atac Imamoglu, Susanne F. Yelin, Mikhail D. Lukin, and J. Ignacio Cirac, Dissipative phase transition in a central spin system, Phys. Rev. A **86**, 012116 (2012).

[14] Mattias Fitzpatrick, Neereja M. Sundaresan, Andy C. Y. Li, Jens Koch, and Andrew A. Houck, Observation of a Dissipative Phase Transition in a One-Dimensional Circuit QED Lattice, Phys. Rev. X **7**, 011016 (2017).

[15] Wim Casteels, Rosario Fazio, and Christiano Ciuti, Critical dynamical properties of a first-order dissipative phase transition, Phys. Rev. A **95**, 012128 (2017).

[16] Fabrizio Minganti, Alberto Biella, Nicola Bartolo, and Cristiano Ciuti, Spectral theory of Liouvillians for dissipative phase transitions, Phys. Rev. A **98**, 042118 (2018).

[17] Thomas Fink, Anne Schade, Sven Höfling, Christian Schneider, and Ataç Imamoglu, Signatures of a dissipative phase transition in photon correlation measurements, Nat. Phys. **14**, 365 (2018).

[18] Myung-Joong Hwang, Peter Rabl, and Martin B. Plenio, Dissipative phase transition in the open quantum Rabi model, Phys. Rev. A **97**, 013825 (2018).

[19] Ralf Bulla, Hyun-Jung Lee, Ning-Hua Tong, and Matthias Vojta, Numerical renormalization group for quantum impurities in a bosonic bath, Phys. Rev. B **71**, 045122 (2005).

[20] Nikolaus Hartman, Christian Olsen, Silvia Lüscher, Mohammad Samani, Saeed Fallahi, Geoffrey C. Gardner, Michael Manfra, and Joshua Folk, Direct entropy measurement in a mesoscopic quantum system, Nat. Phys. **14**, 1083 (2018).

[21] Timothy Child, Owen Sheekey, Silvia Lüscher, Saeed Fallahi, Geoffrey C. Gardner, Michael Manfra, Andrew Mitchell, Eran Sela, Yaakov Kleeorin, Yigal Meir *et al.*, Entropy Measurement of a Strongly Coupled Quantum Dot, Phys. Rev. Lett. **129**, 227702 (2022).

[22] Timothy Child, Owen Sheekey, Silvia Lüscher, Saeed Fallahi, Geoffrey C. Gardner, Michael Manfra, and Joshua Folk, A robust protocol for entropy measurement in mesoscopic circuits, Entropy **24**, 417 (2022).

[23] M. Field, C. G. Smith, Michael Pepper, D. A. Ritchie, J. E. F. Frost, G. A. C. Jones, and D. G. Hasko, Measurements of Coulomb Blockade with a Noninvasive Voltage Probe, Phys. Rev. Lett. **70**, 1311 (1993).

[24] Philip W. Anderson, Infrared Catastrophe in Fermi Gases with Local Scattering Potentials, Phys. Rev. Lett. **18**, 1049 (1967).

[25] I. L. Aleiner, Ned S. Wingreen, and Yigal Meir, Dephasing and the Orthogonality Catastrophe in Tunneling through a Quantum Dot: The "Which Path?" Interferometer, Phys. Rev. Lett. **79**, 3740 (1997).

[26] Baidyanath Misra and E. C. George Sudarshan, The Zeno's paradox in quantum theory, J. Math. Phys. (N.Y.) **18**, 756 (1977).

[27] G. Hackenbroich, B. Rosenow, and H. A. Weidenmüller, Quantum Zeno Effect and Parametric Resonance in Mesoscopic Physics, Phys. Rev. Lett. **81**, 5896 (1998).

[28] See Supplemental Material at http://link.aps.org/supplemental/10.1103/PhysRevLett.131.126502 for further details. which includes Refs. [23,29–33].

[29] László Borda, Gergely Zaránd, Walter Hofstetter, B. I. Halperin, and Jan von Delft, Su(4) Fermi Liquid State and Spin Filtering in a Double Quantum Dot System, Phys. Rev. Lett. **90**, 026602 (2003).

[30] W. Hofstetter and G. Zarand, Singlet–triplet transition in lateral quantum dots: A numerical renormalization group study, Phys. Rev. B **69**, 235301 (2004).

[31] Alexander Altland and Ben D. Simons, *Condensed Matter Field Theory* (Cambridge University Press, Cambridge, England, 2010).

[32] Jan Von Delft and Herbert Schoeller, Bosonization for beginners—Refermionization for experts, Ann. Phys. (Berlin) **510**, 225 (1998).

[33] John Cardy, *Scaling and Renormalization in Statistical Physics* (Cambridge University Press, Cambridge, England, 1996), Vol. 5.

[34] Ian Affleck and Andreas W. W. Ludwig, The Fermi edge singularity and boundary condition changing operators, J. Phys. A **27**, 5375 (1994).

[35] Alexander O. Gogolin, Alexander A. Nersesyan, and Alexei M. Tsvelik, *Bosonization and Strongly Correlated Systems* (Cambridge University Press, Cambridge, England, 2004).

[36] CL Kane, Lectures on bosonization, Boulder Summer School lectures (2005), https://boulderschool.yale.edu/2005/boulder-school-2005-lecture-notes.

[37] Ralf Bulla, Theo A. Costi, and Thomas Pruschke, Numerical renormalization group method for quantum impurity systems, Rev. Mod. Phys. **80**, 395 (2008).

[38] Eran Sela, Yuval Oreg, Stephan Plugge, Nikolaus Hartman, Silvia Lüscher, and Joshua Folk, Detecting the Universal Fractional Entropy of Majorana Zero Modes, Phys. Rev. Lett. **123**, 147702 (2019).

[39] Cheolhee Han, Zubair Iftikhar, Yaakov Kleeorin, Anne Anthore, Frédéric Pierre, Yigal Meir, Andrew K. Mitchell, and Eran Sela, Fractional Entropy of Multichannel Kondo Systems from Conductance-Charge Relations, Phys. Rev. Lett. **128**, 146803 (2022).

[40] David R. Nelson and J. M. Kosterlitz, Universal Jump in the Superfluid Density of Two-Dimensional Superfluids, Phys. Rev. Lett. **39**, 1201 (1977).

[41] D. Cevik, Manuel Gadella, Ş Kuru, and Javier Negro, Resonances and antibound states for the Pöschl-Teller potential: Ladder operators and SUSY partners, Phys. Lett. A **380**, 1600 (2016).

[42] Katarzyna Macieszczak, Emanuele Levi, Tommaso Macrì, Igor Lesanovsky, and Juan P. Garrahan, Coherence, entanglement, and quantumness in closed and open systems with conserved charge, with an application to many-body localization, Phys. Rev. A **99**, 052354 (2019).

[43] Zhanyu Ma, Cheolhee Han, Yigal Meir, and Eran Sela, Symmetric inseparability and number entanglement in charge-conserving mixed states, Phys. Rev. A **105**, 042416 (2022).

[44] Cheolhee Han, Yigal Meir, and Eran Sela, Realistic Protocol to Measure Entanglement at Finite Temperatures, Phys. Rev. Lett. **130**, 136201 (2023).